

# Double fragmentation in cation radicals. An example in the NADH analogues series

Agnès Anne, Sylvie Fraoua, Jacques Moiroux\* and Jean-Michel Savéant\*

Laboratoire d'Electrochimie Moléculaire de l'Université Denis Diderot, Unité Mixte de Recherche Université, CNRS No. 7591, 2 Place Jussieu, 75251 Paris Cedex 05, France

Received 5 November 1997; revised 8 January 1998; accepted 3 February 1998

**ABSTRACT:** The cation radical of 9-*tert*-butyl-*N*-methylacridan, generated electrochemically or photochemically, offers, in the presence of strong bases, a remarkable example of a double fragmentation. Whereas in acidic or weakly basic media the *tert*-butyl radical is cleaved with concomitant formation of the methylacridinium cation, the presence of a strong base triggers the cleavage of both the methyl group borne by the nitrogen atom and the *tert*-butyl group on C-9 leading to acridine, formaldehyde and the *tert*-butyl anion, even though methylacridinium cation is stable under these conditions. The origin of this unprecedented behavior resides in the prior deprotonation of the methyl group borne by the nitrogen atom which outruns the usual deprotonation at the 9-carbon because this is slowed by the steric hindrance due to the presence of the *tert*-butyl group. © 1998 John Wiley & Sons, Ltd.

**KEYWORDS:** double fragmentation; cation radicals; NADH analogues

## INTRODUCTION

The chemistry of cation radicals attracts sustained attention in connection with their importance in organic and biological processes. Anodic oxidations are also currently analyzed in terms of cation radical chemistry.<sup>1ab</sup> The reactions of ion radicals fall into two categories, one in which they react as radicals, the other in which they react as Lewis and/or Brønsted acids (cation radicals) or as Lewis and/or Brønsted bases (anion radicals).<sup>1c</sup> Coupling of the unpaired electrons in the encounter of two ion radicals leading to a dimer is one of the most typical reactions of the first type. Concerning cation radicals, such reactions are of crucial importance in the dynamics of the first stages of electropolymerizations leading to conductive polymers.<sup>2</sup> Reaction with a nucleophile, yielding, after deprotonation, anodic substitution products is one of the reactions of the second type.<sup>3</sup> Deprotonation may also be the first step of cation radical transformation<sup>4–6</sup> leading to a radical that may be further oxidized or undergo carbon–carbon or carbon–heteroatom bond fission. Another possibility is that carbon bond fragmentation occurs in the first stage of the cation radical evolution as, for example, in the case of *tert*-butylated analogues of NADH.<sup>7</sup>

In the same series of compounds we have found still another type of transformation, namely the cleavage of

one carbon–nitrogen bond and of one carbon–carbon (or carbon–oxygen) bond triggered by the initial deprotonation of the cation radical.

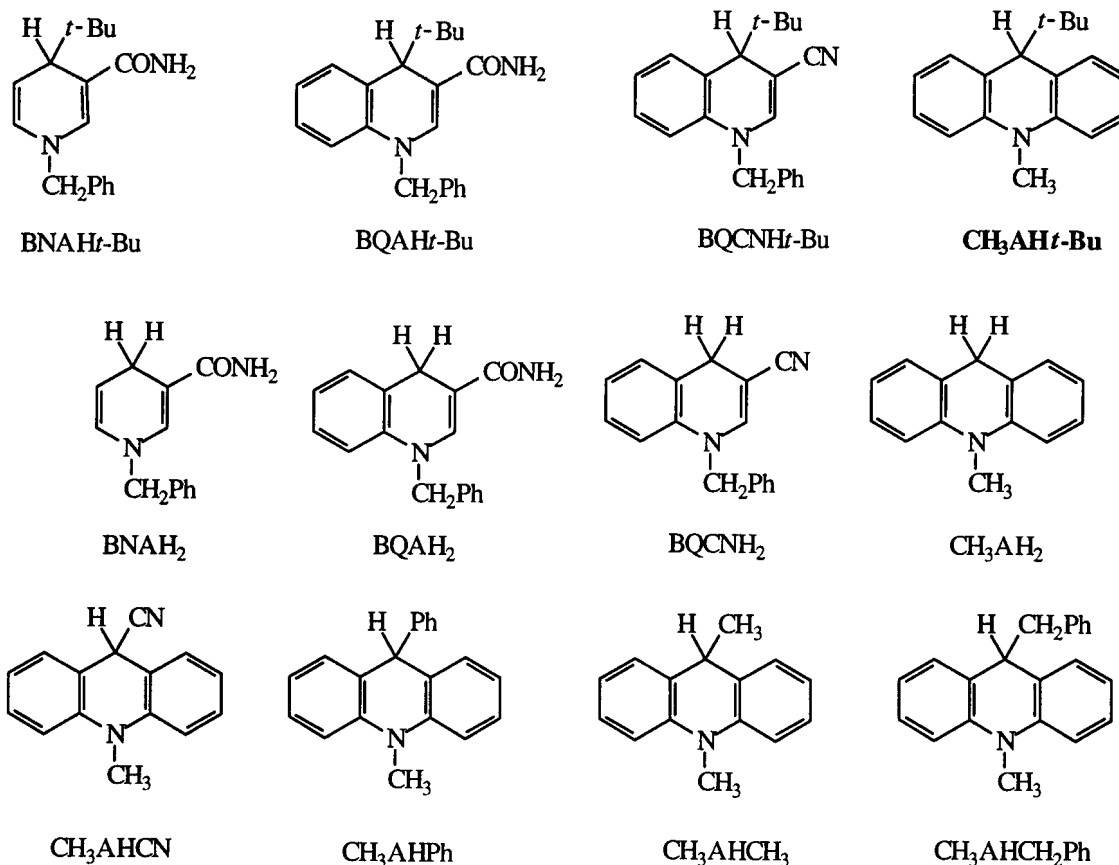
NADH analogues belong to the general class of dihydropyridines. An analysis of single and double fragmentation reactions in cation radicals of dihydropyridines may be important for a better understanding of the mechanism of metabolism of these compounds by cytochrome P450 which opposes their use as calcium antagonists.<sup>8</sup>

The compound we have investigated in this respect is CH<sub>3</sub>AH*t*-Bu (Chart I).

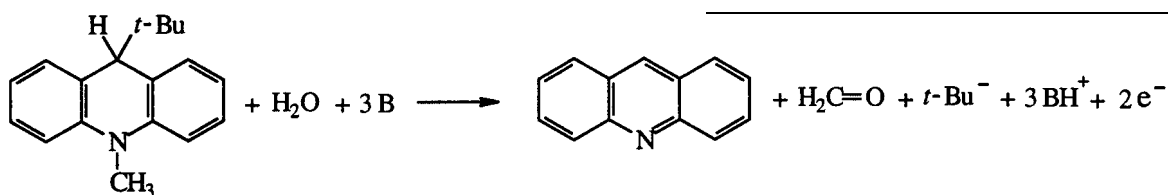
## RESULTS AND DISCUSSION

With the exception of CH<sub>3</sub>AH*t*-Bu, the electrochemically generated cation radicals of all the *tert*-butyl derivatives illustrated undergo a C–*t*-Bu cleavage, yielding the *t*-Bu<sup>•</sup> radical and the pyridinium cation, AH<sup>+</sup>, whatever the pH of the solution.<sup>7a</sup> With CH<sub>3</sub>AH*t*-Bu, the formation of *t*-Bu<sup>•</sup> and of the 10-methylacridinium cation, CH<sub>3</sub>AH<sup>+</sup>, was also observed, albeit only in acidic media, namely between pH 9.4 and 14.7. In the presence of bases of higher p*K*<sub>a</sub> starting with collidine (2,4,6-trimethylpyridine, p*K*<sub>a</sub> = 15.6), a different behavior was observed. It has been shown earlier that the cation radicals of 9-substituted acridans, CH<sub>3</sub>AHR (R = Ph, CH<sub>3</sub>, CH<sub>2</sub>Ph<sup>6b,c</sup> and CN<sup>6d</sup>) do not undergo any C–C cleavage but rather deprotonate in the presence of a base to yield the corresponding radicals, CH<sub>3</sub>AR<sup>•</sup>, and, after a second

\*Correspondence to: J. Moiroux or J.-M. Savéant, Laboratoire d'Electrochimie Moléculaire de l'Université Denis Diderot, Unité Mixte de Recherche Université, CNRS No. 7591, 2 Place Jussieu, 75251 Paris Cedex 05, France.



electron transfer, the  $\text{CH}_3\text{AR}^+$  cation. The cation radicals of all the  $\text{AH}_2$  derivatives illustrated also deprotonate at C-9 in the presence of a base.<sup>6b,c</sup> One would have therefore expected that  $\text{CH}_3\text{AHt-Bu}^{+\bullet}$  would deprotonate, yielding  $\text{CH}_3\text{At-Bu}^\bullet$  and eventually  $\text{CH}_3\text{At-Bu}^+$ , when the pH becomes high enough for this reaction to outrun the extrusion of the  $t\text{-Bu}^\bullet$  radical. In fact, a different behavior was observed, namely the formation of acridine and formaldehyde corresponding to the following overall reaction:



$\text{CH}_3\text{AHt-Bu}^{+\bullet}$  can be generated electrochemically or photochemically. Its UV-visible spectrum obtained by laser pulse photolysis in the presence of an oxidative quencher ( $\text{CCl}_4$ ) is as shown in Fig. 1. The initial formation of the cation radical in electrochemical experiments can be detected by means of cyclic voltammetry where a one-electron reversible wave is observed upon raising the scan rate even in the most basic media (the scan rate required to observe the reversibility

goes up to  $500\text{ V s}^{-1}$  with the strongest base). The standard potential of the  $\text{CH}_3\text{AHt-Bu}/\text{CH}_3\text{AHt-Bu}^{+\bullet}$  couple derived from these experiments as the mid-point between the anodic and cathodic peak potentials is  $0.910\text{ V vs SCE}$ . These observations prove that the cation radical is indeed the initial intermediate of the sequence of reactions leading to the formation of acridine.

At low scan rates ( $\nu < 1\text{ V s}^{-1}$ ), in the presence of a strong base ( $\text{p}K_a \geq 15.6$ ), a two-electron irreversible anodic wave is observed (Fig. 2, full line) which shifts in

the negative direction upon increasing the concentration of base. The quasi-reversible wave appearing upon scan reversal (re-reduction followed by re-oxidation) is the same as the wave obtained with a solution containing only protonated acridine besides the supporting electrolyte. These observations contrast with the behavior that is found in the absence of base (Fig. 2, dotted line). The irreversible anodic wave is significantly smaller. The re-reduction wave is irreversible and has a different location

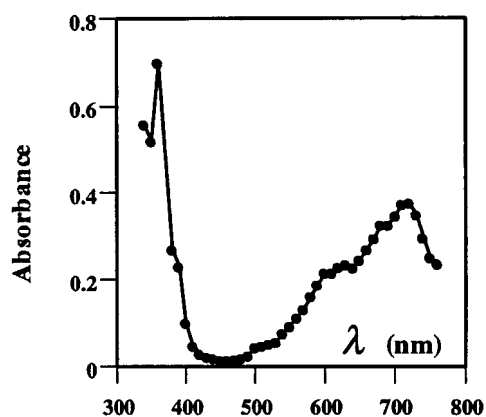
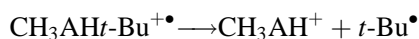


**Figure 1.** Absorption spectrum of  $\text{CH}_3\text{AH}t\text{-Bu}^{+\bullet}$  in acetonitrile recorded 1 ms after the pulse.  $\text{CH}_3\text{AH}t\text{-Bu}$  (0.16 mM) + 0.1%  $\text{CCl}_4$ ; 120 mJ laser pulse at 308 nm

and shape. It corresponds to the reduction of the  $\text{CH}_3\text{AH}^+$  cation formed upon extrusion of  $t\text{-Bu}^\bullet$  radical as discussed earlier:<sup>7a</sup>



Protons are produced upon further oxidation of the products. Since there is no base present in the solution other than the starting molecule,  $\text{CH}_3\text{AH}t\text{-Bu}$ , this is partly protonated and thus partly inactivated toward oxidation, thus explaining why the anodic wave is smaller in the absence of base than in the presence of a strong base. In the presence of a weak base, the same cleavage of the cation radical occurs but the peak height corresponds to two electrons per molecule and the peak potential does not depend on the concentration of base.

Turning back to the case of a strong base, strong indications exist at this stage that acridine is the main reaction product and that the sequence of reactions that eventually lead to this product starts with the initial formation of the cation radical, immediately followed by a step in which the added base is involved. It is also worth noting that the  $\text{CH}_3\text{AH}^+$  cation is stable in the presence of the strong bases used here.<sup>9</sup> Therefore, the reaction triggered by the latter is not merely the conversion into acridine of the  $\text{CH}_3\text{AH}^+$  cation that would be formed initially.

More information on product distribution was gained at the preparative scale. A potential-controlled electrolysis of a solution containing 2.18 mM  $\text{CH}_3\text{AH}t\text{-Bu}$ , 0.2 M 2,4,6-trimethylpyridine and 0.1 M  $\text{Bu}_4\text{NBF}_4$  in acetonitrile was carried out at 1.0 V vs SCE at a platinum grid working electrode. Aliquots were assayed by means of cyclic voltammetry during the course of the electrolysis. Electrolysis was stopped when the height of the anodic peak due to the oxidation of the remaining  $\text{CH}_3\text{AH}t\text{-Bu}$  was *ca* 10% of its original value. The number of electrons exchanged was found to be 2.1, in agreement with cyclic voltammetry (Fig. 2). The resulting composition of the

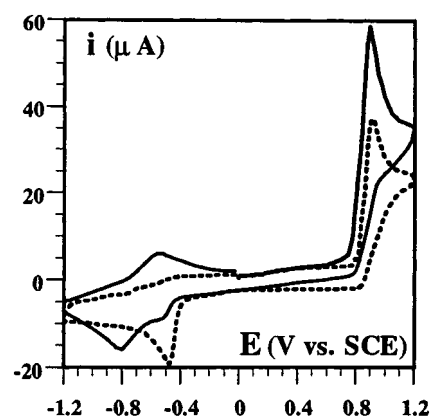


**Figure 2.** Cyclic voltammograms of  $\text{CH}_3\text{AH}t\text{-Bu}$  (2 mM) in the absence (dotted line) and presence (full line) of a strong base (0.17 M 2,4,6-trimethylpyridine) in acetonitrile + 0.1 M  $\text{Bu}_4\text{NBF}_4$  at 20°C. Successive potential scans from 0 to 1.2 V, from 1.2 to -1.2 V and from -1.2 to 0 V at  $\nu = 0.2 \text{ V s}^{-1}$

electrolyzed solution is reported in Table 1 (under the heading 'CV assay'). The species that could be assayed through their anodic or cathodic peaks under such conditions are  $\text{CH}_3\text{AH}t\text{-Bu}$ , *N*-methylacridane ( $\text{CH}_3\text{AH}_2$ ), acridine, *N*-methylacridone,  $\text{CH}_3\text{AH}^+$  and the dimer  $(\text{CH}_3\text{AH})_2$  resulting from the one-electron reduction of  $\text{CH}_3\text{AH}^+$ .<sup>10</sup>

High-performance liquid chromatography (HPLC) was also used to analyze the electrolyzed solution (see Experimental section). The yields thus found are reported in Table 1 (under the heading 'HPLC assay'). The agreement between the CV and the HPLC assays is satisfactory.

The main product is acridine. However, a small amount of  $\text{CH}_3\text{AH}^+$  is still found, indicating that the  $t\text{-Bu}$  extrusion reaction that occurs in the absence of base, or presence of weak bases, still competes, albeit to a small extent.

The HPLC analysis of a solution of 0.16 mM  $\text{CH}_3\text{AH}t\text{-Bu}$  and 0.2 M 2,4,6-trimethylpyridine in acetonitrile after one laser pulse irradiation was also carried out. As can be

**Table 1.** Distribution of products in the electrochemical and photochemical oxidation of  $\text{CH}_3\text{AH}t\text{-Bu}$  in the presence of 2,4,6-trimethylpyridine

| Compound                          | Controlled-potential electrolysis |                | Laser flash photolysis: HPLC assay (%) |
|-----------------------------------|-----------------------------------|----------------|--|
|                                   | CV assay (%)                      | HPLC assay (%) |  |
| $\text{CH}_3\text{AH}t\text{-Bu}$ | 11                                | 8              | 93                                     |
| $\text{CH}_3\text{AH}^+$          | 13                                | 11             | 2                                      |
| $(\text{CH}_3\text{AH})_2$        | 0                                 | 0              | 0                                      |
| $\text{CH}_3\text{AH}_2$          | 0                                 | 0              | 0                                      |
| Acridine                          | 75                                | 73             | 3.5                                    |
| <i>N</i> -Methylacridone          | 0                                 | 0              | 0                                      |

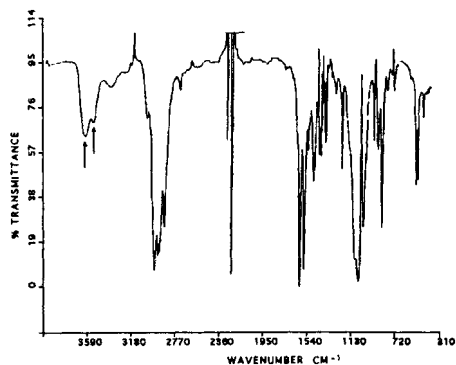


**Figure 3.** IR spectrum of a solution containing initially 1.92 mM  $\text{CH}_3\text{AHt-Bu}$ , 0.1 M  $\text{Bu}_4\text{NBF}_4$  and 0.35 M 2,4,6-trimethylpyridine in acetonitrile electrolyzed at a controlled potential of 1.0 V vs SCE until the concentration of the acridine produced is 1.1 mM. The arrows indicate two of the bands that reveal the presence of formaldehyde and whose heights can be used to determine the formaldehyde concentration (see text)

seen in Table 1, acridine is again produced, even if the conversion to products is small in these experiments.

The formation of acridine implies the oxidative extrusion of the methyl group from the nitrogen atom. We therefore looked for formaldehyde among the reaction products. The IR spectrum of the electrolyzed solution is shown in Fig. 3. The two bands at 3548 and 3616  $\text{cm}^{-1}$  are absent in the spectrum of a solution containing only  $\text{CH}_3\text{AHt-Bu}$ ,  $\text{CH}_3\text{AH}^+$ , acridine and 2,4,6-trimethylpyridine, introduced in acetonitrile at the same concentrations as those given by the CV or HPLC assays. The absorbance at 1610  $\text{cm}^{-1}$  is also markedly smaller. Addition of formaldehyde brings about the appearance of the two bands at 3548 and 3616  $\text{cm}^{-1}$  and a significant increase in the absorbance at 1610  $\text{cm}^{-1}$ . Obviously  $\text{H}_2\text{CO}$  is produced in the electrochemical oxidation of  $\text{CH}_3\text{AHt-Bu}$  in the presence of 2,4,6-trimethylpyridine. Plots of the peak heights at 3548 and 3616  $\text{cm}^{-1}$  vs  $\text{H}_2\text{CO}$  concentration in the 0–2 mM range give two calibration curves showing that both peak heights are roughly proportional to the  $\text{H}_2\text{CO}$  concentration over this range. Using the calibration curves, the  $\text{H}_2\text{CO}$ : acridine ratio is  $0.85 \pm 0.05$ , a result proving that the observed demethylation eventually produces  $\text{H}_2\text{CO}$ .

The CV oxidation wave of  $\text{CH}_3\text{AHt-Bu}$  in the presence of a strong base passes from a two-electron irreversible behavior to a one-electron reversible behavior upon raising the scan rate. We may use this variation of the peak height to investigate the kinetics of the reaction of the cation radical with the base. The variations of the peak current with the scan rate and the base concentration are displayed in Fig. 4. They fit well with a 'DISP1' mechanism<sup>1c</sup> such as that depicted in Scheme 1 in which it is assumed that the reaction of the base with the cation radical involves a deprotonation of the methyl group borne by the nitrogen. The values of the deprotonation rate constants thus obtained are summarized in Table 2.

**Table 2.** Rate constants of deprotonation of  $\text{CH}_3\text{AHt-Bu}^{\bullet+}$  by strong bases<sup>a</sup>

| Base <sup>b</sup>       | $\text{p}K_{\text{a,BH}^+}^{\text{c}}$ | $\text{Log}k^{\text{d}}$ | $\text{Log}k^{\text{e}}$ | $\text{Log}(k_{\text{H}}/k_{\text{D}})^{\text{f}}$ |
|-------------------------|--|--------------------------|--------------------------|--|
| 2,4,6-Trimethylpyridine | 15.6                                   | 2.7                      | <4.5                     |  |
| Benzylamine             | 16.8                                   | 4.6                      | 5.0                      | 0.6  |
| <i>tert</i> -Butylamine | 18.1                                   | 4.7                      | 5.1                      | 0.6  |
| Piperidine              | 18.9                                   | >5.4                     | 6.8                      |  |

<sup>a</sup> In acetonitrile at 20 °C

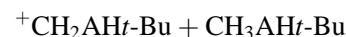
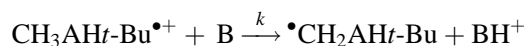
<sup>b</sup>  $15 < [B] < 150$  mM, in buffered or unbuffered medium.

<sup>c</sup> From Refs<sup>7b</sup> and<sup>11</sup>.

<sup>d</sup> Cyclic voltammetric determination, uncertainty =  $\pm 0.2$ .

<sup>e</sup> Laser flash photolysis determination ( $[\text{CH}_3\text{AHt-Bu}] = 0.16$  mM, 0.1%  $\text{CCl}_4$ ), uncertainty =  $\pm 0.2$ .

<sup>f</sup> Cyclic voltammetric determination, uncertainty =  $\pm 0.3$ .



**Scheme 1**

The kinetics of the reaction of  $\text{CH}_3\text{AHt-Bu}^{\bullet+}$  with strong bases may also be followed by the decrease of its UV–visible spectrum with time after generation by a laser pulse in the presence of an oxidative quencher ( $\text{CCl}_4$ ). At 660 nm,  $\text{CH}_3\text{AHt-Bu}^{\bullet+}$  absorbs appreciably right after the pulse (see Fig. 1) and the absorbance decreases to zero with increasing time. First-order kinetics are obeyed, the pseudo first-order rate constant

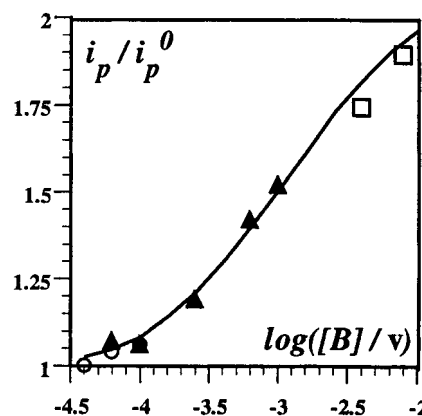
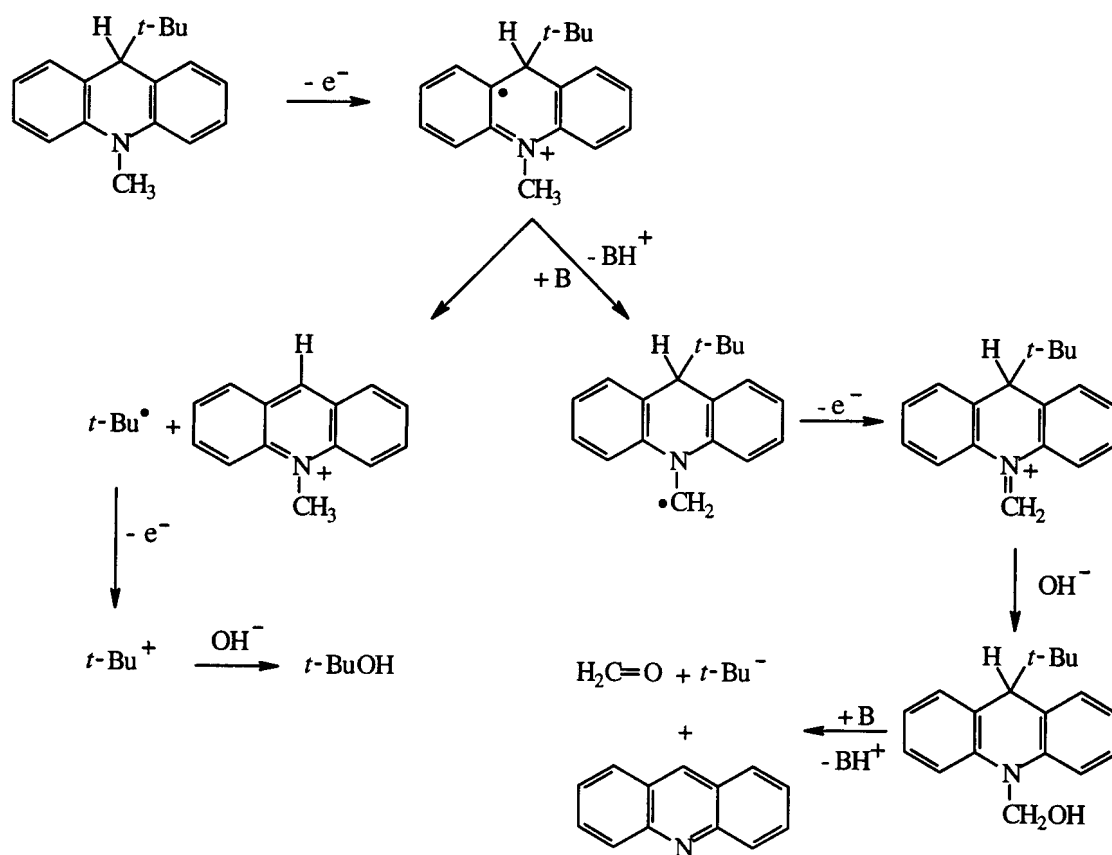


**Figure 4.** Variation of the rate constant of the reaction between  $\text{CH}_3\text{AHt-Bu}^{\bullet+}$  obtained from the oxidation of  $\text{CH}_3\text{AHt-Bu}$  (3 mM) and *tert*-butylamine (concentration in mM) in acetonitrile + 0.5 M  $\text{Et}_4\text{NBF}_4$ . Scan rate,  $v$ , in  $\text{V s}^{-1}$ .  $[B] = 12.4$  mM ( $\circ$ ), 81.6 mM ( $\blacktriangle$ ), 150 mM ( $\square$ ). The solid line represents the theoretical variation of  $i_p/i_p^0$  ( $i_p$  is the peak current and  $i_p^0$  the peak current for a one-electron reversible transfer) for a DISP1 mechanism with  $k = 10^{4.7} \text{ l mol}^{-1} \text{ s}^{-1}$  (see text)



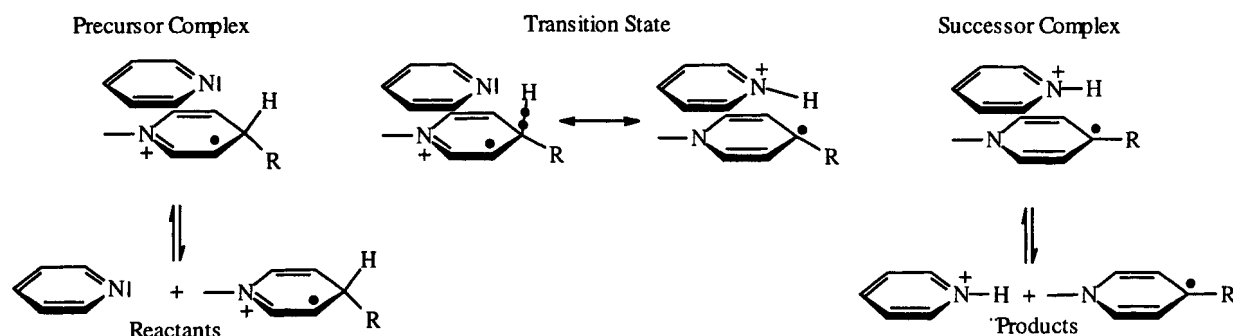
being proportional to the concentration of the strong base as already observed for the deprotonation of cation radicals of other NADH analogues, using the same technique.<sup>6</sup> The resulting second-order rate constants are reported in Table 2. The agreement between the rate constants derived from cyclic voltammetry and laser flash photolysis is satisfactory in the range where each of the two techniques could be used.

In order to prove that the base does deprotonate the cation radical at the methyl borne by the nitrogen atom, as depicted in Scheme 1, we investigated the kinetic isotope effect resulting from the replacement of N-CH<sub>3</sub> by N-CD<sub>3</sub>. As can be seen in Table 2, there is indeed a significant kinetic isotope effect, confirming that the deprotonation of the cation radical at the methyl borne by the nitrogen atom is the rate-determining step of the reaction eventually leading to acridine and formaldehyde.

The preceding observations thus lead to the reaction mechanism depicted in Scheme 2. Instead of the last step of Scheme 2, one could envisage that the 9-*tert*-butyl-*N*-hydroxymethylacridan would decompose to CH<sub>2</sub>O and acridan and that the latter would be oxidized to acridine. This pathway would, however, consume two additional electrons, leading to a total electron stoichiometry of 4. The very fact that the electron stoichiometry is only 2 implies that the *tert*-butyl group is expelled as an anion. *t*-Bu<sup>-</sup> may react with any proton donor present to give 2-

methylpropane or with the acetonitrile solvent to give 2-imino-3,3-dimethylbutane or a polymer. As reported in the Experimental section, all attempts to identify 2-methylpropane or 2-imino-3,3-dimethylbutane (or 2-keto-3,3-dimethylbutane after addition of water) by means of gas-phase chromatography (GPC) and IR absorption spectroscopy, respectively, were unsuccessful. The cleavage of *t*-Bu<sup>-</sup> probably initiates the anionic oligomerization of solvent molecules, explaining why the solution turns purple during the electrolysis in the presence of 2,4,6-trimethylpyridine (unbuffered medium) or orange in a buffered medium (2,4,6-trimethylpyridine plus HClO<sub>4</sub>).

The next question to be addressed is why deprotonation of CH<sub>3</sub>AH*t*-Bu<sup>•+</sup> involves the methyl borne by the nitrogen atom rather than the hydrogen borne by C-9 as it does with CH<sub>3</sub>AH<sub>2</sub><sup>•+</sup>, CH<sub>3</sub>AHPh<sup>•+</sup>, CH<sub>3</sub>AHCH<sub>3</sub><sup>•+</sup> and CH<sub>3</sub>AHCH<sub>2</sub>Ph<sup>•+</sup>. It has already been noted that the intrinsic barrier for the deprotonation of these cation radicals at the C-9 position increases in the indicated order as a consequence of steric hindrance according to the representation given in Scheme 3<sup>6c</sup> (for clarity, the lateral benzene rings of CH<sub>3</sub>AHR and the substituents on pyridine have been omitted). The steric effect arises at the level of the successor complex and causes the intrinsic barrier to increase while the precursor complex and the transition state remain approximately unchanged. One



Scheme 3

may therefore suggest that, with a *tert*-butyl group in the 9-position, steric hindrance is large enough for the competing N-CH<sub>3</sub> deprotonation to become the preferred pathway, thus triggering the sequence of reactions depicted in Scheme 2. It is interesting in this connection that deprotonation at the N-CH<sub>3</sub> group has previously been observed in the case of CH<sub>3</sub>AH<sub>2</sub> in photochemical experiments. The sensitizer being a ketone or a quinone, the photogenerated basic center, viz. the anionic oxygen of the ketyl radical, is thus located much closer to the N-CH<sub>3</sub> group and than to C-9 in the radical ion pair resulting from the photoelectron transfer reaction.<sup>12</sup>

## CONCLUSIONS

The cation radical of CH<sub>3</sub>AH*t*-Bu can be generated electrochemically or photochemically. In acidic or weakly basic media it undergoes the elimination of the *tert*-butyl radical, forming the CH<sub>3</sub>AH<sup>+</sup> cation. In the presence of strong bases, it offers a remarkable example of a double fragmentation involving the extrusion of both the methyl group borne by the nitrogen atom and the *tert*-butyl group on C-9 leading to acridine, formaldehyde and the *tert*-butyl anion. The origin of this unprecedented behavior resides in the prior deprotonation of the methyl group borne by the nitrogen atom which outruns the usual deprotonation at C-9 which is slowed by the steric hindrance caused by the presence of the *tert*-butyl group.

## EXPERIMENTAL

**Chemicals.** The various methylacridane derivatives were prepared according to previously described procedures, CH<sub>3</sub>AH*t*-Bu,<sup>7c</sup> CD<sub>3</sub>AH*t*-Bu,<sup>6d</sup> (CH<sub>3</sub>AH)<sub>2</sub>,<sup>10</sup> CH<sub>3</sub>AH<sup>+</sup> and CH<sub>3</sub>AH<sub>2</sub>.<sup>13</sup> All other chemicals were obtained from Aldrich and were of the highest purity available. They were used as received.

**Instruments and procedures.** They were the same as described previously for cyclic voltammetry, electrolysis<sup>10</sup> and laser flash photolysis.<sup>6d</sup> The optical pathlength for UV-visible spectrophotometric detection was 2 mm.

HPLC assays were performed as follows. Aliquots (20 μl) of the reaction mixture were injected on to a reversed-phase Hypersil C<sub>18</sub>; ODS2 column. The mobile phases were (A) 80:20 methanol-water + 10 mM Na<sub>2</sub>HPO<sub>4</sub> and (B) methanol. The gradient consisted of a 5 min isocratic step with 100% A, followed by a 7 min isocratic step with 100% B and a 5 min linear step returning to the initial conditions. The flow-rate was 1.0 ml min<sup>-1</sup>. The chromatographic peaks were identified by UV spectrophotometry at 290 and/or 342 nm by comparison with authentic samples. Quantitation of acridine (*t<sub>r</sub>* = 5.4 min), AHCH<sub>3</sub><sup>+</sup> (*t<sub>r</sub>* = 6.4 min) and unreacted *t*-BuAHCH<sub>3</sub> (*t<sub>r</sub>* = 14.9 min) was derived from integrated peak vs concentration calibration curves.

In IR absorption measurements the cell thickness, between CaF<sub>2</sub> windows, was 0.5 mm. Calibration curves showed that the peak heights at 3548 and 3616 cm<sup>-1</sup> were proportional to the formaldehyde concentration in the range 0–2 mM. Searching evidence for the possible production of 2-imino-3,3-dimethylbutane, we proceeded as follows. Water (2 mM) was added to the electrolyzed solution to hydrolyze the imine to 2-keto-3,3-dimethylbutane, which exhibits characteristic IR absorption bands at 3000, 1700, 1450, 1350 and 1140 cm<sup>-1</sup>. We did not detect the appearance of any of those bands.

In order to obtain evidence for the possible production of 2-methylpropane, the electrolysis was carried out in a cell sealed with septa. Both the electrolyzed solution and the gas phase above it were analyzed by means of GPC. A Porapak Q column 80–100 mesh of 2 m length (Alltech), was used in an oven at 70 °C with helium under a pressure of 4 bar as the carrier gas and a thermal conductivity detector. The retention times of 2-methylpropane, *n*-butane and acetonitrile were 12.5, 15 and 21 min, respectively. Injections of 10 μl of the solution and 500 μl of the gas phase gave no peaks at 12.5 or 15 min.

## Acknowledgment

We are indebted to Alain Adenier for his help with FTIR spectroscopy.

## REFERENCES

- (a) S. D. Ross, M. Finkelstein and E. J. Rudd, *Organic Chemistry*, Vol. 32, pp. 211–218. Academic Press, New York (1975); (b) H. Lund and M. M. Baizer, *Organic Electrochemistry*, Marcel Dekker, New York (1991); (c) C. P. Andrieux and J.-M. Savéant, in *Investigations of Rates and Mechanisms of Reactions; Techniques of Chemistry*, edited by C.F. Bernasconi, Vol. 6, 4th Edition, Part 2, pp. 305–390. Wiles, New York (1986).
- (a) G. B. Street, in *Handbook of Conducting Polymers*, edited by T.A. Skotheim. Vol. 1, pp. 265–291. Marcel Dekker, New York (1986); (b) for kinetic studies on the early stages of the electropolymerization of pyrroles, see C. P. Andrieux, P. Audebert, P. Hapiot and J.-M. Savéant, *J. Phys. Chem.*, **95**, 10158–10164 (1991).
- (a) L. Ebersson, *Adv. Phys. Org. Chem.* **18**, 79–185 (1982); (b) V. D. Parker, *Acc. Chem. Res.* **17**, 243–250 (1984); (c) U. C. Yoon and P. S. Mariano, *Acc. Chem. Res.* **25**, 233–240 (1992); (d) for more recent work, see M. S. Workentin, L. J. Johnston, D. D. M. Wayner and V. D. Parker, *J. Am. Chem. Soc.* **116**, 8279–8287 (1994), and references cited therein.
- (a) For a review on fragmentation of photochemically generated cation radicals, see A. Albini, M. Mella and M. Freccero, *Tetrahedron* **50**, 575–607 (1994).
- (a) See Refs 4(a) and (b)–(d) and references cited therein; (b) E. Bacciochi, T. Del Giaco and F. Elisei, *J. Am. Chem. Soc.* **115**, 12280–12289 (1993); (c) B. Karki, J. P. Dinnocenzo, J. P. Jones and K. R. Korzekwa, *J. Am. Chem. Soc.* **117**, 3657–3664 (1995); (d) F. D. Lewis, D. M. Bassani, E. L. Burch, B. E. Cohen, J. A. Engleman, G. D. Reddy, S. Schneider, W. Jaeger, P. Gedeck and M. Gahr, *J. Am. Chem. Soc.* **117**, 660–669 (1995); (e) X. Zhang, S. R. Yeh, Hong, M. Freccero, A. Albini, D. E. Falvey and P. S. Mariano, *J. Am. Chem. Soc.* **116**, 4211–4220 (1994); (f) V. D. Parker and M. Tilset, *J. Am. Chem. Soc.* **113**, 8778–8781 (1991); (g) L. M. Tolbert, R. K. Khanna, E. Popp, L. Gelbaum and L. A. Bottomley, *J. Am. Chem. Soc.* **112**, 2373–2378 (1990).
- (a) With the cation radicals of NADH analogs, Brønsted plots have been obtained using a wide range of opposing bases. The  $pK_a$ s of the cation radicals could be derived from experimental data, hence allowing the determination of the intrinsic barriers,  $6b^{\text{e}}$  which is seldom the case in cation radical deprotonation studies; (b) A. Anne, P. Hapiot, J. Moiroux, P. Neta and J. M. Savéant, *J. Phys. Chem.* **95**, 2370–2377 (1991); (c) A. Anne, P. Hapiot, J. Moiroux, P. Neta and J. M. Savéant, *J. Am. Chem. Soc.* **114**, 4694–4701 (1992); (d) A. Anne, S. Fraoua, P. Hapiot, J. Moiroux and J. M. Savéant, *J. Am. Chem. Soc.* **117**, 7412–7421 (1995); (e) A. Anne, S. Fraoua, V. Grass, J. Moiroux and J. M. Savéant, *J. Am. Chem. Soc.* **120**, 2951–2958 (1998).
- (a) S. Fukuzumi, Y. Tokuda, T. Kitano, T. Okamoto and J. Otera, *J. Am. Chem. Soc.* **115**, 8960–8968 (1993); (b) A. Anne, J. Moiroux and J. M. Savéant, *J. Am. Chem. Soc.* **115**, 10224–10230 (1993); (c) A. Anne, S. Fraoua, J. Moiroux and J. M. Savéant, *J. Am. Chem. Soc.* **118**, 3938–3945 (1996); (d) For carbon–carbon fragmentation in other cation radicals, see (e)–(j) references therein; the sequencing of deprotonation C–C cleavage is not always obvious;<sup>7j</sup> (e) P. Maslak, *Top. Curr. Chem.* **168**, 1–46 (1993); (f) P. Maslak, T. M. Vallombroso, W. H. Chapman and J. N. Narvaez, *Angew. Chem., Int. Ed. Engl.* **33**, 73–75 (1994); (g) L. Chen, M. S. Farahat, H. Gan, S. Farid and D. G. Whitten, *J. Am. Chem. Soc.* **117**, 6398–6399 (1995); (h) H. Gan, U. Lenhos, I. R. Gould and D. G. Whitten, *J. Phys. Chem.* **99**, 3566–3573 (1995); (i) J. H. Horner, F. N. Martinez, O. M. Musa, M. Newcomb and H. Shahin, *J. Am. Chem. Soc.* **117**, 11124–11135 (1995); (j) R. D. Burton, M. D. Bartberger, Y. Zhang, J. R. Eyler and K. S. Schanze, *J. Am. Chem. Soc.* **118**, 5655–5664 (1996).
- (a) J. S. Lee, N. E. Jacobsen and P. R. Ortiz de Montellano, *Biochemistry* **27**, 7703–7710 (1988); (b) F. P. Guengerich, W. R. Brian, M. Iwasakei, M. A. Sari, C. Bäärnhielm and P. Berntsson, *J. Med. Chem.* **34**, 1838–1844 (1991).
- A. Anne and J. Moiroux, *J. Org. Chem.* **55**, 4608–4614 (1990).
- A. Anne, P. Hapiot, J. Moiroux and J. M. Savéant, *J. Electroanal. Chem.* **331**, 959–970 (1992).
- (a) G. Cauquis, A. Deronzier, D. Serve and E. Vieil, *J. Electroanal. Chem.* **60**, 205–215 (1975); (b) I. M. Kolthoff, M. K. Chantoni and S. Bhowmik, *J. Am. Chem. Soc.* **90**, 23–28 (1968); (c) J. F. Coetzee, *Prog. Phys. Org. Chem.* **4**, 76–77 (1967).
- (a) K. S. Peters, E. Pang and J. Rudzki, *J. Am. Chem. Soc.* **104**, 5535–5537 (1982); (b) L. E. Manning and K. S. Peters, *J. Am. Chem. Soc.* **107**, 6452–6458 (1985).
- R. M. G. Roberts, D. Ostovic and M. M. Kreevoy, *Faraday Discuss. Chem. Soc.* **74**, 257–265 (1982).